Carbohydrate Polymers 83 (2011) 1279–1284

Contents lists available at ScienceDirect

Carbohydrate Polymers

journal homepage: www.elsevier.com/locate/carbpol

Bacterial cellulose/poly(3-hydroxybutyrate) composite membranes

Hernane S. Barud*, Josiane L. Souza, Daniele B. Santos, Marisa S. Crespi, Clóvis A. Ribeiro, Younés Messaddeq, Sidney J.L. Ribeiro

Institute of Chemistry, São Paulo State University – UNESP, P.O. Box 355, Araraquara, SP 14801-970, Brazil

ARTICLE INFO

Article history:
Received 17 June 2010
Received in revised form 7 September 2010
Accepted 20 September 2010
Available online 4 November 2010

Keywords:
Bacterial cellulose
Poly(3-hydroxybutyrate) (PHB)
Green polymers

ABSTRACT

Bacterial cellulose (BC)/poly(3-hydroxybutyrate) (PHB) composite membranes were prepared from chloroform-swollen BC membranes and PHB chloroform solutions. Relative contents were varied from 25 to 90 wt.% of PHB. Macroscopically homogeneous composite membranes were characterized by scanning electron microscopy, Fourier-transformed infrared spectroscopy, X rays diffraction, thermal analysis and stress–strain measurements. Depending on the relative compositions membranes coating of BC microfibrils by PHB and PHB precipitation inside the BC 3D network of cellulose fibers could be observed. Improved mechanical properties were observed for the composites compared to the individual components suggesting potential applications for the new biodegradable materials.

1. Introduction

Composite materials based on fibers-reinforced polymeric matrix are important for structural applications where a combination of high strength and stiffness, durability and relatively low weight are key requirements (Marck, 1999). Research efforts are being harnessed in developing fully biodegradable "green" composites prepared in a sustainable way (Yang, Wang, & Wang, 2007) and cellulose and polyhydroxyalkanoates (PHA) based composites will be certainly important in this field due to their intrinsic biodegradability and biocompatibility properties.

Cellulose is the most abundant natural biopolymer on Earth, being synthesized by plants and also by some bacteria species. The "not so green" implications involved in cellulose extraction from plants and trees can be overcome with the employment of bacterial cellulose (BC) (Barud et al., 2007; Gardner, Oporto, Mills, & Samir, 2008; Klemm et al., 2006).

In particular *Gluconacetobacter xylinus* bacteria produces cellulose markedly different from plant cellulose. From the culture medium, a pure-cellulose network free of lignin and hemicellulose is obtained as highly hydrated pellicles, composed of a random assembly of ribbon-shaped fibers less than 100 nm wide (Klemm, Heublein, Fink, & Bohn, 2005). The resulting particular supramolecular structure of hydrated BC displays high mechanical strength and a high surface area formed by porous structures that have been an attractive template for inorganic particle stabilization (Barud, de Assunção, et al., 2008; Barud, Barrios, et al., 2008). It is being also considered in the preparation of "green" polysaccharides composites (Grande et al., 2009), thermoplastic biofibers (Gao, Zhang, & Wan, 2010), and different types of synthetic polymers by cross linking reaction with organic monomers (Kramer et al., 2006).

Polyhydroxyalkanoates (PHA), on the other side, are a family of intracellular biopolymers synthesized by bacteria as intracellular carbon and energy storage granules. Among the PHA polymers family, poly-3-hydroxybutyrate (PHB) is produced by *Ralstonia eutropha*. PHB is a biocompatible, biodegradable and thermoplastic polymer, with the plastic-like properties offering the possibility for potential replacement of non-degradable polymers currently used as polyethylene and polypropylene. PHB has a high melting temperature (~175 °C) and thermal instability and brittleness have been the main disadvantages in potential applications (Chandra & Rutsgi, 1998; Dawes & Senior, 1973; Gomez & BuenoNetto, 1997; Knowles, Hastingsh, & Niwan, 1992; Luengo, García, Sandoval, Naharo, & Olivera, 2003; Nonato, Mantelatto, & Rossell, 2001).

In order to improve these properties it is possible to prepare PHB based composites and blends with environmentally degradable polymers (Marck, 1999; Koller & Owen, 1996; Souza, Santos, Crespi, and Ribeiro 2007). PHB/PLA (poly-lactic acid) blends have been studied by DSC, wide-angle X ray diffraction (WAXD) and IR microspectroscopy techniques. These blends are observed to be composed of two immiscible components and the crystalline structures of the individual parts are kept in the final materials (Furukawa et al., 2007). Rheo-optical FTIR spectroscopy technique was applied in order to study the orientation of both polymers chains under stress (Vogel, Hoffmann, & Siesler, 2009). PLA chains were observed to orient parallel to the elongation direction while PHB chains align perpendicularly to the drawing direction. This

* Corresponding author. Tel.: +55 1633016636; fax: +55 1633016636.
E-mail address: hernane.barud@gmail.com (H.S. Barud).

0144-8617/$ – see front matter © 2010 Elsevier Ltd. All rights reserved.
doi:10.1016/j.carbpol.2010.09.049

phenomenon has been interpreted with a continuum mechanical orientation model of lamellar PHB domains within the positively oriented PLA matrix (Vogel et al., 2009).

Poly(3-hydroxybutyrate/hydroxyapatite) composites have been used for bone tissue repair (Liu & Wang, 2007). PHB/maize starch blends are applied for package (Reis et al., 2008; Vinhas, Almeida, & Lima, 2007) and Poly(3-hydroxybutyrate)/chitosan/ketoprofen composites microparticles have been used in controlled drug release in Bazzo, Lemos-Senna, and Pires (2009).

PHB/cellulose esters blends have been studied in Scandola, Ceccorulli, and Pizzoli (1992). Totally miscible amorphous blends were obtained for PHB content up to 50%. PHB was observed to crystallize for higher contents.

Biocomposite double-layer films using PHB and cellulose paper were prepared in Jiang, Morelius, Zhang, and Wolcott (2008). Diminutions in moisture and water absorption and also in the surface roughness were observed in comparison with cellulose paper. The possibility of obtaining a biodegradable material with improved barrier and mechanical properties was clearly demonstrated.

The copolymer poly(3-hydroxybutyrate-co-hydroxyvalerate) (PHBV) is also being used, showing better mechanical properties than PHB (Satyanarayana, Arizaga, & Wypych, 2009). PHBV-cellulose nanowhiskers composites were studied in Cyras, Commisso, Mauri, and Vaizquez (2007). Homogeneous dispersion of the whiskers was achieved with composites displaying improved tensile strength and modulus and increase glass transition temperature.

In this paper we are interested in the preparation and characterization of "green" composites based on bacterial cellulose (BC) and polyhydrohybutyrate (PHB). Composites have been characterized by SEM-FEG microscopy, XRD analysis and FTIR spectroscopy. The thermal behavior and mechanical properties of the BC/PHB composites were also considered.

2. Experimental

Bacterial cellulose membranes and PHB granules were supplied by the Brazilian companies Fibrocel Produtos Biotécnlógicos Ltda and PHB Industrial S/A respectively.

Hydrated (99% water) BC membranes (4 mm thick) were previously submitted to a solvent exchange process by 48 h soaking sequentially in ethanol, acetone and finally chloroform. The resulting chloroform-swollen BC membranes were utilized for the composite preparation.

PHB homopolymer pellets were dissolved in boiling chloroform in closed vials and stirring for 20 h. Solutions were then transferred to Petri Plate's containing the chloroform-swollen BC membranes and the composite membranes were left to dry at room temperature for 12 h. Composite membranes were prepared with the following compositions (PHB wt.%): 25, 50, 70, and 90.

2.1. SEM characterization

Scanning electron microscopy (SEM) images were obtained in a field emission scanning electron microscopy FEI Quanta 200 model. Samples were covered with a 10 nm thick gold layer.

2.2. XRD analysis

XRD patterns were obtained in a Siemens Kristalloflex diffractometer using nickel filtered Cu Kα radiation, with s0.02° step, integration time of 3 s, from 4° to 70° (2θ angle).

2.3. Thermal behavior

DSC curves were obtained from 10 mg of the samples in a 2910-TA Instruments from 40 to 600 °C under nitrogen atmosphere (50 mL min^{-1}) in sealed aluminum pans.

Thermal degradation was followed using a TA 2960 SDT, TA Instruments in the 40–450 °C temperature range in open alumina reference and sample pans under dynamic nitrogen atmosphere (flow rate: 50 mL min^{-1}) and at heating rate of 20 °C min^{-1}.

2.4. Stress–strain

The mechanical measurements were performed at 27 °C with a Dynamic Mechanical Analyzer (DMA) 2980 (TA Instruments) equipped with a film tension clamp. Specimens dimensions were 30.50 mm × 6.20 mm × 0.15 mm (length × width × thickness). A preload force of 0.01 N and force ramp of 8 N m^{-1} were applied until the rupture of sample. The device was previous calibrated and a total of 10 measurements were performed for each sample.

2.5. FTIR spectra

Infrared absorption spectra were obtained from 4.000 to 400 cm^{-1}, with 4 cm^{-1} spectral resolution and 64 scans. KBr pellets were analyzed in a FTIR Spectrum 2000 Perkin-Elmer spectrometer.

3. Results and discussion

Macroscopically homogenous membranes (~150 μm thick) were obtained for all BC/PHB composites. Pure BC and composite membranes appear transparent-milky and white respectively.

3.1. SEM characterization

Fig. 1 shows representatives SEM images of a PHB film obtained by casting from the chloroform solution, a freeze-dried BC membrane, and the 50% PHB composite.

Fig. 1(a) presents the surface image of the pure PHB film. Microparticles are observed on a compact, smooth and uniform structure. Images obtained for pure BC membrane (Fig. 1(b)), reveals the ultrafine network structure composed of a random assembly of ribbon-shaped cellulose fibers less than 100 nm wide (Barud, de Araujo, et al., 2008).

Fig. 1(c) and (d) shows images obtained for the 50% PHB sample. BC microfibrils appear well recovered by PHB. The cross-section image for this same sample, Fig. 1(e) and (f), shows BC microfibrils domains and PHB micro-pellets wrapped by BC microfibrils.

The images allow suggesting that PHB solutions filled BC pores leading to PHB pellets precipitation inside the BC microfibrils network.

3.2. XRD analysis

Fig. 2 shows XRD patterns. Broad diffraction peaks are observed at 15° and 22.5° for the pure BC membrane (Fig. 2(a)). These peaks are assigned to the characteristic interplane distances of cellulose 1_α and 1_β phases ($1\,0\,0_{1\alpha}$, $1\,1\,0_{1\beta}$ and $0\,1\,0_{1\beta}$ planes at 15° and $1\,1\,0_{1\alpha}$ and $2\,0\,0_{1\beta}$ at 22.5°) (Antonniete, 1997; Wadda & Okano, 2001). Fig. 2(b) shows the diffraction pattern obtained for the PHB. Main peaks are observed at $2\theta = 13.5°$ and 16.9°. Broader peaks can be observed at 19.9°, 21.5°, 22.5°, 25.5° and 27.15°. These diffraction lines can be attributed to the orthorhombic PHB lattice (Thiré, Ribeiro, & Andrade, 2006).

Diffraction patterns obtained for the composite membranes show only the cellulose peaks with a decrease intensity for the peak

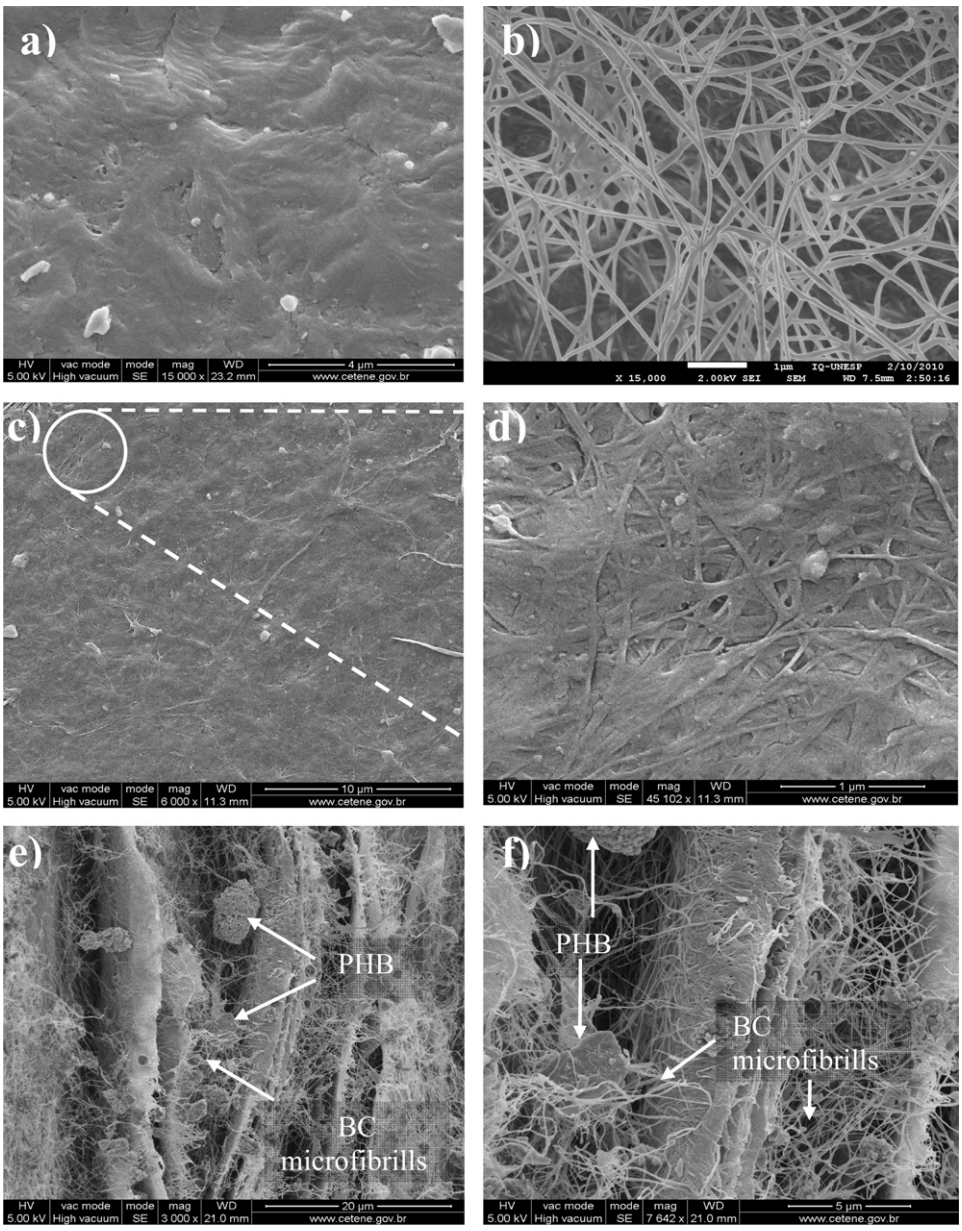

Fig. 1. SEM images of: (a) PHB film; (b) freeze dried BC membrane; (c) and (d) surface image of BC/PHB 50%; (e) and (f) cross-section image of 50% PHB sample.

at 15° for compositions up to 50% PHB (Fig. 2(c) and (d)). For samples 70% and 90% PHB the PHB peaks are clearly observed. Cellulose peaks are hardly observed, specially the 15° one. The 22.5° cellulose peak at 22.5° appears convoluted with the contribution from PHB peaks. Therefore the PHB composite counterpart appears well crystallized for samples 75% and 90%. A similar behavior has been observed for PHB–cellulose esters studied in Scandola et al. (1992) where amorphous PHB is observed for relative contents below 50% in weight. Cellulose crystallinity seems well affected by the PHB presence due to the dramatic change in relative intensity between the 15° and 22.5°.

3.3. FTIR spectroscopy

Fig. 3(I) and (II) shows relevant regions of FTIR spectra. The mains bands observed for pure bacterial cellulose (Fig. 3(I-a) and (II-a)) can be assigned to OH stretching (3454 cm^{-1}), H-bonds (3237 cm^{-1}), CH stretching of CH_2 and CH_3 groups (2902–2717 cm^{-1}), water OH bending (1650 cm^{-1}), CH_2 symmetric bending (1432 cm^{-1}), CH bending (1368 cm^{-1}), antisymmetric bridge C–O–C stretching (1162 cm^{-1}), skeletal vibrations involving C–O stretching (1114–1058 cm^{-1}), antisymmetric out-of-phase stretching (896 cm^{-1}) and OH out-of-phase bending (666–619 cm^{-1}) (Barud, de Assunção, et al., 2008).

The main bands observed in the PHB spectrum (Fig. 3(I-b) and (II-b)) are assigned to C—O stretching (1282 cm^{-1}) and C=O stretching (1730 cm^{-1}), peaks at 2853 cm^{-1}, 2926 cm^{-1} and 2972 refer to C—H stretching and the peak at 3437 cm^{-1} refers to hydroxyl end groups (Zhang, Deng, Zhao, & Huang, 1997).

Spectra obtained for composites display basically the bands observed for the two individual components weighted by the relative contents. OH region between 3000 and 3500 cm^{-1} appears affected by the relative content of the two components that could be related to the change in cellulose crystallinity observed in XRD measurements. However further measurements with a higher number of samples and including different spectroscopic techniques (Raman scattering for example) would be necessary to clarify that question.

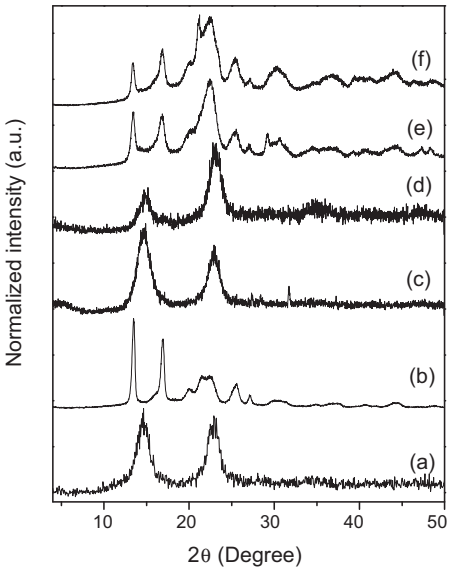

Fig. 2. XRD analyses of: (a) BC; (b) PHB; (c) 25% PHB; (d) 50% PHB; (e) 70% PHB; (f) 90% PHB.

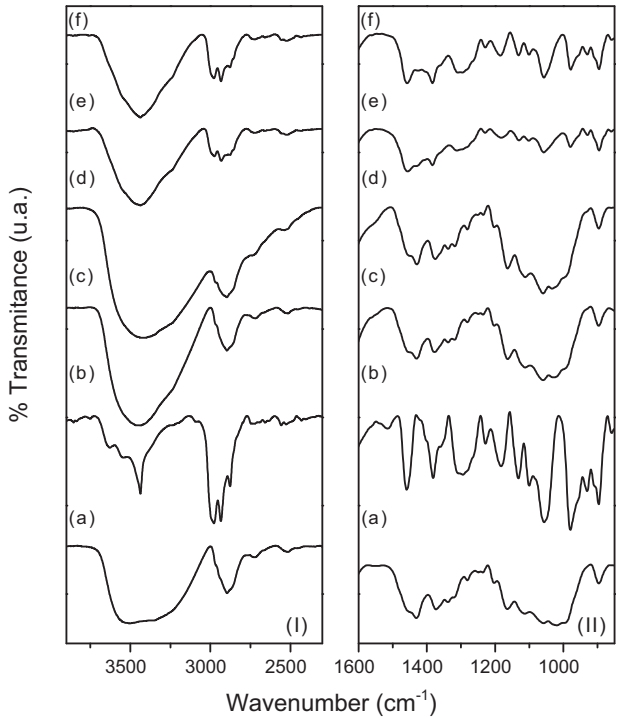

Fig. 3. FTIR spectra of: (a) BC; (b) PHB; (c) 25% PHB; (d) 50% PHB; (e) 70% PHB; (f) 90% PHB.

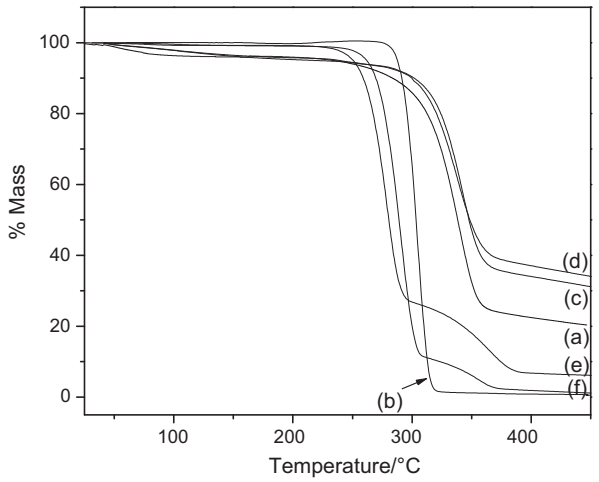

Fig. 4. TG curves for: (a) BC, (b) PHB, (c) 25% PHB, (d) 50% PHB, (e) 70% PHB 70% and (f) 90% PHB.

3.4. Thermal behavior

Fig. 4 shows TG results. The curve obtained for the pure BC membrane (Fig. 4(a)) shows two significant events of weight loss. The first gradual one involving 5% mass loss occurs from room temperature up to 200 °C and can be associated with loss of surface residual solvent; the second one, observed around 330 °C, is attributed to BC pyrolysis. A residue of 20% of carbonaceous materials is observed.

TG curve observed for PHB (Fig. 4(b)) shows only one weight loss starting at around 280 °C up to 320 °C due the thermal decomposition of PHB. Almost no residue is observed (Shahosseini, 2004).

TG curves obtained for BC/PHB composites containing 25 and 50% of PHB (Fig. 4(c) and (d)) display a composition of the events observed for the pure composite components. A continuous mass loss of around 5% is observed from room temperature up to around 250 °C. After that a second important event is observed starting at around 260 °C up to 360 °C which is a temperature higher than the temperature observed for pure PHB. The residue mass was observed to depend on the PHB relative content. 30% mass residue is observed for the sample containing 25% PHB and 35% mass residue is observed for the sample containing 50% PHB.

TG curves obtained for BC/PHB composites containing 70 and 90% of PHB (Fig. 4(e) and (f)) show behavior approaching the one obtained for pure PHB with the main mass loss occurring at lower temperature from around 240 °C to 300 °C. The residue approaches zero with increasing PHB content. Table 1 shows results obtained from TG and DSC curves.

DSC results are shown in Fig. 5. BC shows an endothermic peak starting at low temperature and extending up to 150 °C. As stated in the analysis of TG results this event is related to solvent and bonded water loss. The broad exothermic peak around 350 °C (T_{onset} = 293 °C) is attributed to the partial pyrolysis with fragmentation of carbonyl and carboxylic bonds from anhydrous

Table 1
DSC results, melting point (T_m), enthalpy (ΔH), crystallinity index (% cryst) to the PHB melting peak, and initial decomposition; mass loss temperature (%) data from TG curves.

Sample	PHB melting			Decomposition	Mass loss (%)/temperature (°C)		
	T_m (°C)	ΔH (kJ/g)	% cryst	T_{onset} (°C)			
BC				293(exo)	4.1/200	–/–	73.5/400
PHB	159/173	83.1	57.8	285(endo)	0.3/200	98.3/325	–/–
BC/PHB 25%	167	–	–	307(exo)	4.2/200	–/–	61.7/400
BC/PHB 50%	167	1.2	0.7	304(exo)	4.8/200	–/–	58.2/400
BC/PHB 70%	159/171	28.3	20.1	253(endo)	0.8/200	73.5/310	19.0/400
BC/PHB 90%	159/173	63.8	43.0	268(endo)	0.9/200	88.6/315	9.6/400

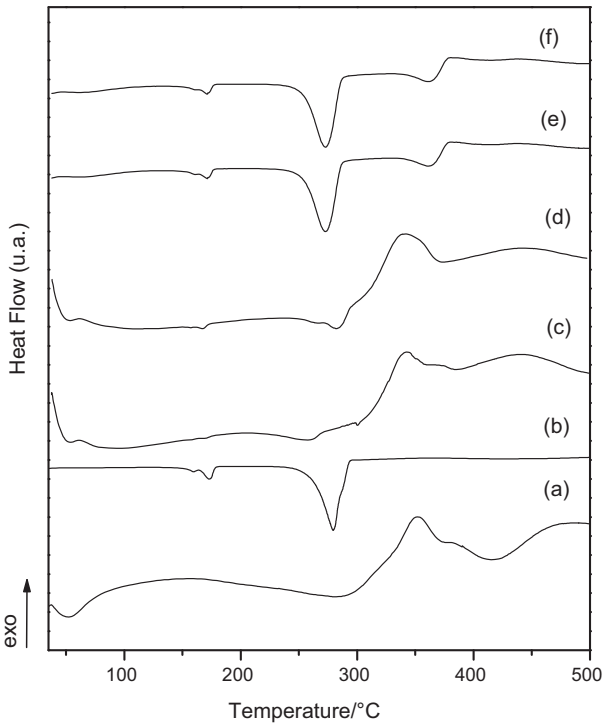

Fig. 5. DSC curves of: (a) BC membrane; (b) PHB film; (c) 25% PHB; (d) 50% PHB; (e) 70% PHB and (f) 90% PHB.

glucose units producing carbon and/or carbon monoxide (Gomez & BuenoNetto, 1997).

The curve obtained for pure PHB shows sharp endothermic events peaking at 170 and 279 °C, related to PHB melting and decomposition respectively.

The BC/PHB composites (Fig. 5(c) and (d)) with 25 and 50% PHB show the same endothermic event related to water-solvent loss observed for pure BC, starting at room temperature and extended up to 150–200 °C. The small endothermic peak around 167 °C refers to melting of the low content of crystalline PHB (Luengo et al., 2003; Scandola et al., 1992). This event is more evident for the composites with higher PHB contents (70 and 90%). As suggested from XRD measurements not only the PHB increasing relative content is responsible for the DSC behavior. Also the low crystallinity of the PHB counterpart observed for samples up to 50% PHB should be considered.

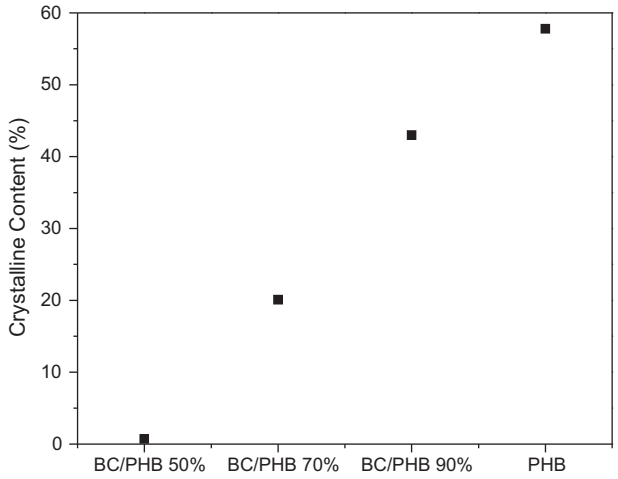

Fig. 6. PHB crystalline content (%) for pure PHB and BC/PHB composites.

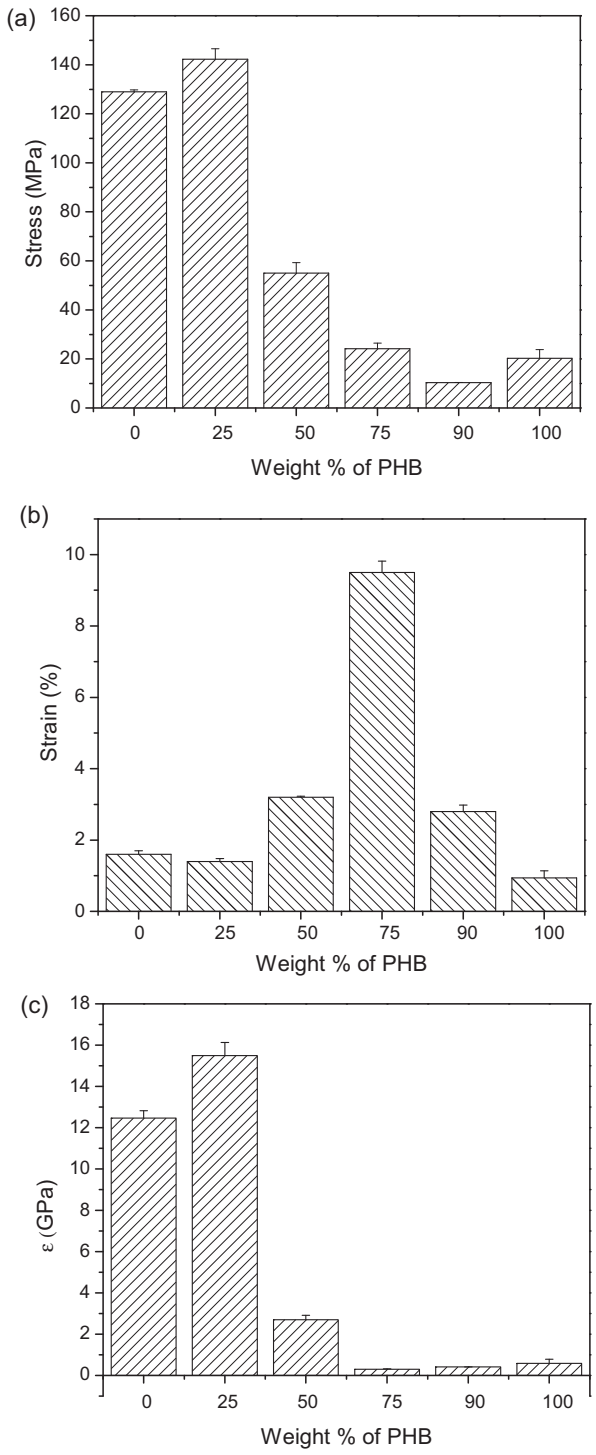

Fig. 7. (A) Tensile strength, (B) elongation at break and (C) Young's modulus of: (a) BC; (b) BC/PHB 25%; (c) BC/PHB 50%; (d) BC/PHB 70%; (e) BC/PHB 90%; (f) PHB film.

Events related to BC are hardly observed for the curves obtained for the composites containing 70% and 90% PHB. Curves closely resemble the one obtained for pure PHB. The endothermic events between 250 and 300 °C refer to the thermal decomposition of PHB. The exothermic one between 300 and 400 °C refer to BC decomposition. The presence of PHB causes change in the thermal stability of BC, leading to a shift of around 10 °C for composite membranes when compared to the pure BC one.

The relative content of crystalline PHB in the composites can be determined using the known fusion heat value (ΔH_0) for a 100% crystalline sample, 146 J/kg (Rosa, Filho, Chui, Calil, & Guedes, 2002). Fig. 6 shows the results. The crystalline PHB content is almost 0% for composites containing up to 50% PHB. Increasing crystallinity if observed with increasing PHB content, confirming that PHB crystallize inside of BC microfibrils for samples above 50% PHB.

3.5. Mechanical tests

The tensile strength, elongation at break and Young modulus of the BC membrane, PHB film, and BC/PHB composites are shown in Fig. 7.

Comparing with the values observed for pure BC, the tensile strength and the Young's Modulus experiment a small increase with the addition of 25% PHB. Pure BC membrane presents a tensile strength of 129 MPa and Young's modulus of 12.5 GPa. The values observed for BC/PHB 25% are 142 MPa for the tensile strength and 15.5 GPa for the Young's modulus. This behavior can be due the good dispersion of PHB into the BC network. The combination of PHB pellets with cellulose networks can result in a denser fiber structure with improved mechanical strength due the good interfacial adhesion and the formation of strong interactions between BC and PHB chains (Fernandes et al., 2009).

The BC/PHB 50% and BC/PHB 70% composites show tensile strength values of 55 MPa and 24 MPa, respectively. These values are lower than the ones observed for pure BC and the composite containing 25% PHB. However these values must be compared with pure PHB that presents tensile strength of 20 MPa. Some reports have in fact shown the efficiency of the three-dimensional network of BC microfibril as good reinforcement for polymers and resins (Fernandes et al., 2009; Kim, Jung, Kim, & Jin, 2009; Yano et al., 2005). Considering that an important drawback concerning practical applications of PHB are the poor mechanical properties, the reinforcement provided by the addition of BC seems to be of potential interest (Marck, 1999).

The BC/PHB 90% composite shows the lowest values of tensile strength for all BC/PHB composites. From XRD analysis and DSC curves, well crystallized PHB phase is observed and this behavior can be related to the observed decrease in tensile strength.

Concerning the elongation at break, values are observed to increase with the addition of PHB up to 70%. Further addition leads to a relative decrease of the elongation.

The lowest value of elongation was observed for pure PHB (0.95%). The largest one was observed for the 70% PHB sample (9.5%).

4. Conclusions

New bacterial cellulose (BC)/poly(3-hydroxybutyrate) (PHB) composites were prepared from chloroform swollen BC membranes obtained from *Gluconacetobacter xylinum* cultures and PHB chloroform solution's. SEM analyses revealed homogeneous coating of BC surface by PHB deposition, and cross-section images showed BC microfibril involving PHB pellets that precipitate inside the BC 3-D network. FTIR and DRX results show that the identity of each counterpart is preserved in the composites. PHB was observed to display lower crystallinity for samples containing up to 50% PHB. Above 50% PHB crsytallinity was observed to increase. The new composites could find important applications since better mechanical properties were observed than for the isolated polymers. Tensile strength as high as 144 MPa, elongation at break of 9.5% and Young's modulus as high as 15.5 GPa were observed by playing with the relative BC and PHB contents.

Acknowledgments

The authors acknowledge Brazilian agencies CNPq, CNPES, FAPESP for financial support. CETENE (Centro de Tecnologias Estratégicas do Nordeste), Recife-PE is also acknowledged for SEM analyses.

References

Antonniete, C. O. (1997). *Cellulose*, *4*, 173–207.
Barud, H. S., Ribeiro, C. A., Crespi, M. S., Martines, M. A., Dexpert-Ghys, J., Marques, R. F. C., et al. (2007). *Journal of Thermal Analysis Calorimetry*, *87*, 815–818.
Barud, H. S., Barrios, C., Regiani, T., Marques, R. F. C., Verelst, M., Ghys, J. D., et al. (2008). *Material Science Engineering*, *28*, 515–518.
Barud, H. S., de Assunção, R. M. N., Martines, M. A. U., Ghys, J. D., Marques, R. F. C., Messaddeq, Y., et al. (2008). *Journal Sol–Gel Science and Technology*, *46*, 363–367.
Barud, H. S., de Araujo, A. M., Jr., Santos, D. B., de Assunção, R. M. N., Meireles, C. S., Cerqueira, D. A., et al. (2008). *Thermochimica Acta*, *471*, 61–69.
Bazzo, G. C., Lemos-Senna, E., & Pires, A. T. N. (2009). *Carbohydrate Polymers*, *77*, 839–844.
Chandra, R., & Rutsgi, R. (1998). *Progress in Polymer Science*, *23*, 1273–1335.
Cyras, V. P., Commisso, M. S., Mauri, A. N., & Vaizquez, A. (2007). *Journal of Applied Polymer Science*, *106*, 749–751.
Dawes, E. A., & Senior, P. J. (1973). *The role and regulation of energy reserve polymers in micro-organisms*. California: Academic Press.
Fernandes, S. C. M., Oliveira, L., Freire, C. S. R., Silvestre, A. J. D., Pascoal Neto, C., Gandini, A., et al. (2009). *Green Chemistry*, *11*, 2023–2029.
Furukawa, T., Sato, H., Murakami, R., Zhang, J., Noda, I., Ochiai, S., et al. (2007). *Polymer*, *48*, 1749–1755.
Gao, J. W. C., Zhang, Y., & Wan, Y. (2010). *Material Science Engineering C*, *30*, 214–218.
Gardner, D. J., Oporto, G. S., Mills, R., & Samir, M. A. S. A. (2008). *Journal of Adhesion Science and Technology*, *22*, 545–567.
Gomez, J. G. C., & BuenoNetto, C. L. (1997). *Revista Brasileira Engineering Química*, *17*, 24–29.
Grande, C. J., Torres, F. G., Gomez, C. M., Troncoso, O. P., Canet-Ferrer, J., & Martínez-Pastor, J. (2009). *Material Science Engineering C*, *29*, 1098–1104.
Jiang, L., Morelius, E., Zhang, J., & Wolcott, M. (2008). *Journal of Composite Materials*, *42*, 2629–2645.
Kim, Y., Jung, R., Kim, H. S., & Jin, H. J. (2009). *Current Applied Physics*, *9*, S69–S71.
Klemm, D., Heublein, B., Fink, H. P., & Bohn, A. (2005). *Angewandte Chemie-International Edition*, *44*, 3358–3393.
Klemm, D., Schumann, D., Kramer, F., Heßler, N., Hornung, M., Schmauder, H. P., et al. (2006). *Advances in Polymer Science*, *205*, 49–96.
Knowles, J. C., Hastingsh, G. W. O., & Niwan, S. B. (1992). *Biomaterials*, *13*, 491–496.
Koller, I., & Owen, A. J. (1996). *Polymer International*, *39*, 175–181.
Kramer, F., Klemm, D., Schumann, D., Hebler, N., Wesarg, F., Fried, W., et al. (2006). *Macromolecular Symposium*, *244*, 136–148.
Liu, Y., & Wang, M. (2007). *Current Applied Physics*, *7*, 547–554.
Luengo, J. M., García, B., Sandoval, A., Naharo, G., & Olivera, E. R. (2003). *Current Opinion in Microbiology*, *6*, 251–260.
Marck, J. E. (1999). *Polymer data handbook*. Oxford: Oxford University Press, Inc.
Nonato, R. V., Mantelatto, T. E., & Rossell, C. E. V. (2001). *Applied Microbiology Biotechnology*, *57*, 1–5.
Reis, K. C., Pereira, J., Smith, A. C., Carvalho, C. W. P., Wellner, N., & Yakimets, I. (2008). *Journal Food Engineering*, *89*, 361–369.
Rosa, D. S., Filho, R. P., Chui, Q. S. H., Calil, M. R., & Guedes, C. G. F. (2002). *European Polymer Journal*, *39*, 233–241.
Satyanarayana, K. G., Arizaga, G. G. C., & Wypych, F. (2009). *Progress in Polymer. Sciene*, *34*, 982–1021.
Scandola, M., Ceccorulli, G., & Pizzoli, M. (1992). *Macromolecules*, *25*, 6441–6446.
Shahosseini, S. (2004). *Process Biochemistry*, *39*, 963–969.
Souza, J. L., Santos, A. F., Crespi, M. S., & Ribeiro, C. A. (2007). *Journal of Thermal Analysis*, *87*, 673–677.
Thiré, R. M. S. M., Ribeiro, T. A. A., & Andrade, C. T. (2006). *Journal of Applied Polymer Science*, *100*, 4338–4347.
Vinhas, G. M., Almeida, Y. M. B., & Lima, M. A. G. A. (2007). *Química Nova*, *30*, 1584–1588.
Vogel, C., Hoffmann, G., & Siesler, H. W. (2009). *Vibrational. Spectroscopy*, *49*, 284–287.
Wadda, M., & Okano, T. (2001). *Cellulose*, *8*, 173–183.
Yang, K. K., Wang, X. L., & Wang, W. Y. (2007). *Journal of Industrial Engineering Chemistry*, *13*, 485–500.
Yano, H., Sugiyama, J., Nakagaito, A. N., Nogi, M., Matsuura, T., Hikita, M., et al. (2005). *Advanced in Materials*, *17*, 153–155.
Zhang, L., Deng, X., Zhao, S., & Huang, Z. (1997). *Polymer International*, *44*, 104–110.